Publ. Astron. Obs. Belgrade No. 102 (2022), 95 - 99 *Contributed Paper*

BOHMIAN DYNAMICS OF POSITRONS CHANNELED THROUGH A CHIRAL CARBON NANOTUBES

M. ĆOSIĆ[1], M. HADŽIJOJIĆ[1] and N. NEŠKOVIĆ[2]

[1]*Laboratory of Physics, "Vinča" Institute of Nuclear Sciences, National Institute of the Republic of Serbia, University of Belgrade, P. O. Box 522, 11001 Belgrade, Serbia*

[2]*World Academy of Art and Science, Napa, California, USA*

E-mail mcosic@vinca.rs

Abstract. The framework of the dynamical system theory was used for studying the dynamics of the quantum positron trajectories channeling through a chiral carbon nanotube. Obtained insight was used to explain the pattern-forming ability of the quantum self-interference.

1. INTRODUCTION

We shall analyze a dynamic of the quasi-parallel positron beam, of energy $E_k = 2$ MeV, transmitting through a chiral single-wall-carbon-nanotube (SWCNT) of chiral indices (11, 9). The circumference of this SWCNT consists of 602 atomic string pairs Saito et al. 1998. Consequently, positron-nanotube interaction potential is axially symmetric. If the linear momentum of the incoming positron is parallel to the SWCNT axis it will undergo through a series of correlated small-angle scatterings. As a result, longitudinally averaged SWCNT potential gently steers trajectories of these so-called *channeled* particles, Gemmell 1974.

Let us introduce Descartes's coordinate axis whose z-axis coincides with the SWCNT's axis. The $y = 0$ cross-section of the SWCNT potential is given by the following expression, (see Artru et al. 2005)

$$V(x) = \frac{8e^2R}{\sqrt{3}\varepsilon_0 l^2}\sum_{s=1}^{3}\alpha_s \begin{cases} I_0\left(\beta_s\dfrac{|x|}{a_{TF}}\right)K_0\left(\beta_s\dfrac{R}{a_{TF}}\right), & \text{for } |x| \le R, \\ K_0\left(\beta_s\dfrac{|x|}{a_{TF}}\right)I_0\left(\beta_s\dfrac{R}{a_{TF}}\right), & \text{for } |x| > R, \end{cases} \tag{1}$$

here e and ε_0 are elementary charge and vacuum permittivity, $R = 0.69$ nm and $l = 0.144$ nm are SWCNT's radius and C-C bond length (see Saito et al. 1998), α_s, β_s, and $a_{TF} = 0.0258$ nm are Molière's universal fitting parameters and

Thomas-Fermi's screening radius of C atom (see Molière 1947), while I_0 and K_0 are modified Bessel's functions of zeroth (Oliver 1972). Since potential $V(x)$ does not depend on the z coordinate, positron dynamics is effectively one-dimensional. Thus, classical trajectories $x(z)$ are solutions to the following Newton's equation

$$m_{\mathrm{p}} \frac{d^2x}{dz^2} = -\frac{1}{v_z^2} \partial_x V(x), \tag{2}$$

where m_{p} is positron's relativistic mass, v_z is its conserved longitudinal velocity. The maximal deflection angle of positron trajectory is given by the following expression $\Theta_c = \sqrt{V(R)/E_k}$ =8.8 mrad called the critical angle [Gemmell]. The quantum trajectories $x_{\mathrm{qu}}(z)$ were obtained in a two-step procedure. In the first step the corresponding Schrödinger equation

$$i\partial_z \psi(x,z) = -\frac{\hbar}{2m_p v_z} \partial_x^2 \psi(x,z) + \frac{1}{\hbar v_z} V(x) \psi(x,z), \tag{3}$$

was solved assuming Gaussian initial state

$$\psi_0(x) = \frac{\sigma_\theta^{1/2}}{(2\pi)^{1/4} \left(\hbar m_{\mathrm{p}} v_z\right)^{1/2}} \exp\left[-\frac{\sigma_\theta^2}{\hbar^2 m_p^2 v_z^2} x^2\right] \tag{4}$$

of very small angular divergence $\sigma_\theta = 0.01\Theta_c$. In the second step, the polar form of the wave function $\psi = \sqrt{\rho(x,z)} \exp\left[\frac{i}{\hbar} S(x,z)\right]$ was used to solve Bohm's equations of motion

$$\frac{\mathrm{d}}{\mathrm{d}z} x_{\mathrm{qu}}(z) = \frac{1}{m_{\mathrm{p}} v_z} \partial_x S\big(x_{\mathrm{qu}}(z), z\big), \tag{5}$$

and to calculate the quantum potential

$$Q(x,z) = -\frac{\hbar^2}{2m_{\mathrm{p}}} \frac{\partial_x^2 \sqrt{\rho(x,z)}}{\sqrt{\rho(x,z)}}. \tag{6}$$

In the end, the quantum dynamics was characterized using finite-length local Lyapunov's exponent defined by the following integral, see Ott 2002

$$\lambda_z\left(x_{\mathrm{qu}}(z)\right) = \frac{1}{m_{\mathrm{p}} z} \int_0^z \partial_x^2 S\big(x_{\mathrm{qu}}(z'), z'\big)\, dz'. \tag{7}$$

2. RESULTS

Figure 1 (a) shows the evolution of classical trajectories obtained by the numerical integration of Eq. (2) using the Runge-Kutta method of the fourth-order elaborated in Press et al. 2007. The dynamics of shown trajectory family is regular since it is one-dimensional Ott 2002. Its nontrivial aspect is the appearance of the cusped caustic

lines labeled $c_1, \ldots c_4$. Caustics separate regions of the $y = 0$ plane whose positron multiplicity locally differs by two see Arnol'd 2004. Thus, positron density is infinite along caustics which dominantly determine the shape of the spatial positron yield.

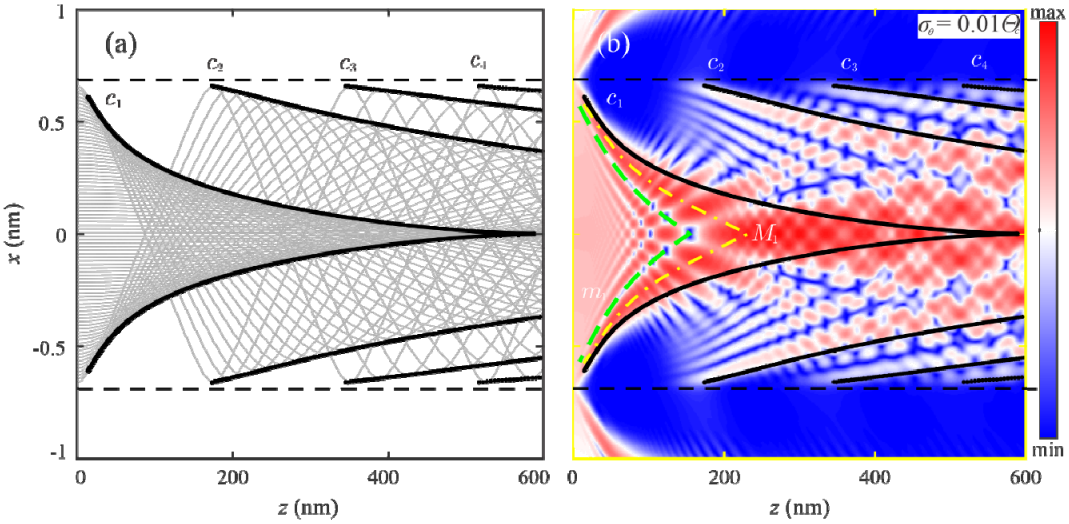

Figure 1: (a) Classical trajectories initially representing parallel beam. (b) Evolution of the quantum positron probability density initially representing quasi-parallel beam. Values of the probability density are color-coded according to the shown colormap. Dashed black lines indicate SWCNT walls. Thick black lines show the classical caustic lines $c_1, \ldots c_4$. The cusped dashed green line and dot-dash yellow lines show lines of dominant maxima and minima M_1 m_1 associated with the caustic c_1.

Figure 1 (b) shows the evolution of the corresponding quantum state obtained by numerical integration of Eq. (3) using Chebyshev's global propagation method, details are in Ćosić et al. 2014. Note accumulation of the probability density on the caustic's side of higher multiplicity see Ćosić et al. 2016. Since total probability is conserved, it cannot have singular maxima. Instead, quantum self-interference creates alternating lines composed of local extrema running "parallel" to the caustics. For simplicity, in Fig. 1(b) only dominant lines labeled $m_1$and M_1 associated with caustic c_1 are specially designated.

The obtained numerical solution enables the study of quantum dynamics in all of its details. However, using it alone, it is very difficult to understand the wave packet's pattern-forming ability. To gain additional insight scientists are often recoursing to the semiclassical approximation, which associates a primitive wave to each classical trajectory, thus reducing every physical effect to the interference of waves arriving at the same location (Berry 1972). Although simple, this approach has several drawbacks. It is difficult to understand pattern formation in regions with no classical trajectories or interference of real and evanescent waves

visible in the region between caustic lines c_1 and c_2 in Fig. 1(b). It cannot be applied in circumstances when positron's de Broglie's wavelength is not negligible, nor when dynamics of the underlying classical system is not regular (Berry 1972).

We shall demonstrate an alternative approach designed to transcend the limitations of the semiclassical approximation. It is known that Bohm's quantum trajectories are always defined and contain the same information as quantum state ψ. Therefore, it is natural to analyze quantum trajectories from the standpoint of the dynamical systems theory and connect it to the wave packet's local focusing generated by the self-interference.

For simplicity, Fig 2(a) shows a subfamily of quantum trajectories occupying the region close to the SWCNT axis, obtained by the numerical integration of Eq. (5) using the Runge-Kutta method of the fourth-order (Press et al. 2007). This Fig. shows that only a few trajectories run across the classical caustic c_1 which represents also a virtual barrier for the quantum trajectories. Note that lines m_1 and M_1 connect together regions repelling and attracting neighboring trajectories the most strongly. Inspection of the quantum potential (6) along the lines m_1 and M_1 reveled that it has very large negative values in the vicinity of the minima while it has moderate values in the vicinity of the maxima. Therefore, the quantum potential is respon-

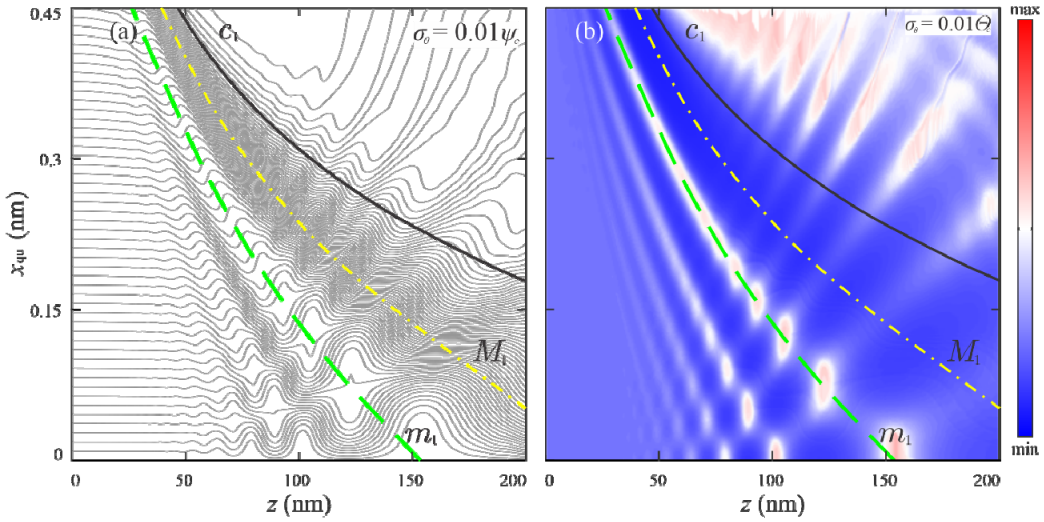

Figure 2: (a) Evolution of the representative subset of the quantum trajectories corresponding to the quantum state shown in Fig. 1 (b). (b) The corresponding distribution of the local finite length Lapunov's exponents. Negative values of the exponents are indicated by different tones of the blue color while positive values are indicated by different tones of the red color. Thich black line shows the classical caustic c_1, while dashed green and dot-dash yellow lines show dominant lines of minima and maxima, m_1 and M_1 respectively associated with caustic c_1.

sible for the creation of regions of strong local repletion of trajectories called repeltors, which explains the exitance of the local destructive self-interference. In this framework, local constructive self-interference is also generated by the action of local repeltors because of the conservation of the total probability.

To characterize the strength of introduced repeltors we have calculated the distribution of the finite-length local Lyapunov's exponents calculated using trapezoidal quadrature (see Press et al. 2007). Figure 2(b) reveals that only some minima are sufficiently low to generate positive islands of Lyapunov's exponents. Closer inspection has confirmed that only those minima have a noticeable influence on the neighboring trajectories. Their basins of repulsion are defined as a zero-level line of Lyapunov's exponent surrounding its positive local maxima.

Since local self-interference is a generic process it can be argued that local repeltors will always appear. Each quantum trajectory can be designated by a list of repeltors it encounters in its evolution. Since in this case evolution of the quantum state is aperiodic evolution of quantum trajectories cannot be periodic. This means that for most trajectories list of encountered repeltors is infinite and aperiodic which according to the information theory has a positive information gain (see Ott 2002) which makes dynamics of Bohmian trajectories in chiral SWCNT weakly complex.

References

Arnol'd, V. I.: 2004, *Catastrophe Theory*, second edition, Berlin: Springer-Verlag.

Artru, X., Fominb, S. P., Shul'ga, N. F., Ispirian, K. A., and Zhevago, N.K.: 2005, *Phys. Rep*. **412**, 89

Berry, M. V., Mount, K.E.: 1972, *Semiclassical approximations in wave mechanics*, Rep. Prog. Phys. **35**, 315.

Ćosić, M., Petrović, S., and Nešković, N.: 2014, *Computational method for the long time propagation of quantum channeled particles in crystals and carbon nanotubes*, Nucl. Instrum. Methods Phys. Res. B, **330**, 33.

Ćosić, M., Petrović, S., and Nešković, N.: 2016, *Quantum primary rainbows in transmission of positrons through very short carbon nanotubes*, Nucl. Instrum. Methods Phys. Res. B, **373**, 52.

Gemmell, D. S.: 1974, Rev. Mod. Phys., **46**, 1.

Molière, G.: 1947, *Z. Naturforschg.*, **2a,** 133

Olver F. W. J.: 1972, 9. *Bessel Functions of Integer Order*, Chap. 9, p. 355 in *Handbook of Mathematical Functions,* edited by Abramowitz, M., and Stegun, I. A., tenth edition, Washington, D.C: National Bureau of Standards.

Ott, E.: 2002, *Chaos in dynamical systems*, second edition, Cambridge: Cambridge University Press.

Press, W. H., Teukolsky, S. A., Vetterling, W. T., and Flannery, B. P.: 2007 *Numerical Recipes*, third edition, Cambridge: Cambridge University Press.

Saito R., Dresselhaus G., and Dresselhaus M. S.: 1998, *Physical Properties of Carbon Nanotubes*, Singapore: Imperial College Press.